JOURNAL OF GEOPHYSICAL RESEARCH, VOL. 95, NO. A8, PAGES 12,187–12,195, AUGUST 1, 1990

Observations on the DE 1 Spacecraft of ELF/VLF Waves Generated by an Ionospheric Heater

H. G. JAMES

Communications Research Centre, Ottawa, Ontario, Canada

U. S. INAN

Space, Telecommunications and Radioscience Laboratory, Stanford University, Stanford, California

M. T. RIETVELD[1]

Max-Planck-Institut für Aeronomie, Katlenburg-Lindau, Federal Republic of Germany

Radio waves at frequencies between 1525 and 5925 Hz were observed on the DE 1 satellite during a pass over the Heating facility of the Max-Planck-Institut für Aeronomie (MPAe Heating) near Tromsø, Norway. The waves were detected during a 2-min period on December 12, 1981, and measurements indicated pulse stretching by a few hundred milliseconds and spectral broadening of about 10 Hz. Measured signal delays are compared with those calculated using three-dimensional ray tracing. The observed signal delays and pulse distortion are not consistent with that expected on the basis of propagation in a smooth magnetosphere between the assumed "polar electrojet antenna" (PEJ) in the ionospheric *D/E* region and the satellite at about 11,000 km altitude. Scattering by density irregularities may be responsible for the observed long delays and spectral broadening, as has been speculated in previous interpretations of spacecraft observations of signals from ground-based ELF/VLF transmitters. Although the MPAe Heating ELF transmissions were 100% square-wave modulated, odd harmonies of the ELF modulation frequencies were not observed at the satellite; this remains unexplained. Similar spectral broadening and signal delays were observed on 10.2-kHz signals from the Omega Norway transmitter during the same DE 1 pass. Using the Omega transmitter as a reference, the PEJ radiated power is estimated to be about 30 W.

1. INTRODUCTION

Investigations using the Heating facility of the Max-Planck-Institut für Aeronomie (MPAe Heating) have successfully demonstrated the generation of extra low frequency (ELF) and very low frequency (VLF) waves by artificial modulation of auroral electrojet currents, sometimes called the polar electrojet antenna (PEJ) [*Stubbe et al.*, 1985]. A significant body of data from ground VLF observations of MPAe Heating has been used to establish the characteristics of downward radiation from the auroral radiator, both near the source [*Rietveld et al.*, 1989, and references therein] and far away [*Barr et al.*, 1986]. The evidence concerning the PEJ radiation as observed from above MPAe Heating is apparently limited to three satellite passes in 1981; AUREOL 3 on December 3 [*Lefeuvre et al.*, 1985]; ISIS 1 on December 9 [*James et al.*, 1984]; and the present DE 1 pass on December 12 [*Inan and Helliwell*, 1985]. The cited literature indicates that the PEJ can sometimes radiate detectable signal levels into the topside ionosphere and nearby magnetosphere. However, some aspects of the satellite observations remain unexplained. The amplitudes measured on ISIS 1 were stronger than implied by simultaneous ground measurements. The harmonic signal ratios of square-wave modulation frequencies were different in space and on the ground [*James et al.*, 1984]. In addition, there remains a general question arising from the MPAe Heating campaign in 1981: why were identifiable transmissions from Heating obtained in only three satellite passes and not in the approximately 20 other similar passes through the magnetosphere near MPAe Heating?

This paper presents a quantitative analysis of DE 1 observations of heater-generated signals. The 11,000-km height of DE 1 at the time of recording is the greatest known distance of observation of ELF/VLF radiation from the PEJ.

Since 1981, research on transionospheric propagation has demonstrated that upward propagating VLF waves can be spectrally broadened [*Bell et al.*, 1983; *Titova et al.*, 1984]. This transionospheric effect is presumed to be due to free-energy sources that either amplify the artificial waves directly or produce irregular density structure which scatters the waves [*Bell and Ngo*, 1988]. Such processes may help to explain the differences between the ground and the ISIS 1 measurements and the low rate of successful observation by satellites of MPAe Heating during the 1981 campaign. We note that a process that modified a transionospherically propagated ELF wave may render it detectable or undetectable in the topside ionosphere.

The important features of the DE 1 observations are long average signal delays, stretching of pulse lengths from 1 s at emission to about 1.5 s at reception, frequency broadening of the received fundamental line, absence of harmonics, and the strengths of the received signals. The first two aspects have been examined in detail using ray tracing in a three-

[1]Now at European Incoherent Scatter Facility, Ramfjordbotn, Norway.

Paper number 90JA01013.
0148-0227/90/90JA-01013$05.00

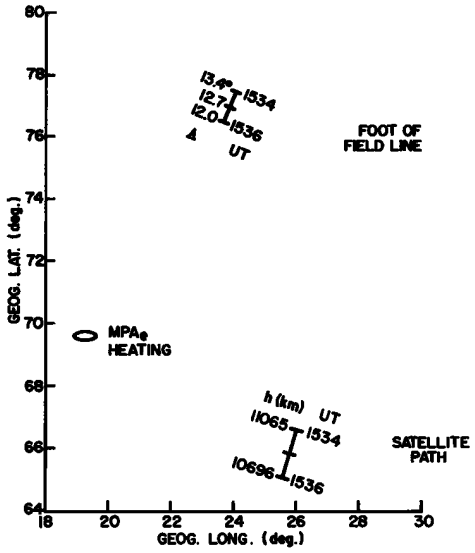

Fig. 1. Subsatellite path of DE 1 during 1534–1536 UT on December 12, 1981. Also shown are the location of MPAe Heating and of the foot of the field lines at 100 km altitude through the spacecraft.

dimensional cold-plasma model of the ionosphere and magnetosphere. The results are described in section 3. Section 4 presents an analysis of the third and fourth observations concerning the frequency spectra, which is also partly based on geometric-optics results. Section 4 also discusses the received signal strengths. In addition, we present some comparisons of the distortion and power levels of signals from the PEJ antenna and from the navigational transmitter Omega Norway. Many of the observed features appear to be attributable to the modification of the ELF/VLF signals due to scattering during their upward transionsopheric propagation.

2. General Results

The DE 1 spacecraft detected ELF/VLF waves during approximately 1534–1536 UT on December 12, 1981, at an altitude of 11,000 km. The geographic positions of the spacecraft during the interval, of MPAe Heating, and of the feet of the field lines through the spacecraft are plotted in Figure 1. The invariant latitudes and altitudes of the spacecraft are also shown. The ELF/VLF signals were detected on the 200-m tip-to-tip dipole antenna that rotated at a rate of 9.87 rpm in the spacecraft equatorial plane [*Shawhan et al.*, 1981]. The spin axis was within a few degrees of the orbit plane normal.

MPAe Heating had a 12-s duty cycle, starting at 0., 12., 24., 36., and 48. s UT, ±0.1 ms, in each UT minute. The 2.759-MHz heater carrier was 100% amplitude modulated with a square ELF/VLF wave. Modulation frequencies of 525, 1525, 2225, 2925, 4425, and 5925 Hz were used, each for 1 s duration. The 12-s HF format was composed of 6 s with X mode right-hand polarization and then 6 s with left-hand O mode. The heater had an effective radiated power of 270 MW in its beam, which had a diameter referred to the 3-dB points of about 30 km at *E* layer heights.

Dynamic spectra of the signals recorded by the wideband receiver of DE 1 [*Gurnett and Inan*, 1988] are shown in Figure 2. The period includes 10 s of continuous data. The X mode heater polarization produced VLF lines that were 7–8 dB stronger than the O mode lines. This predominance of the

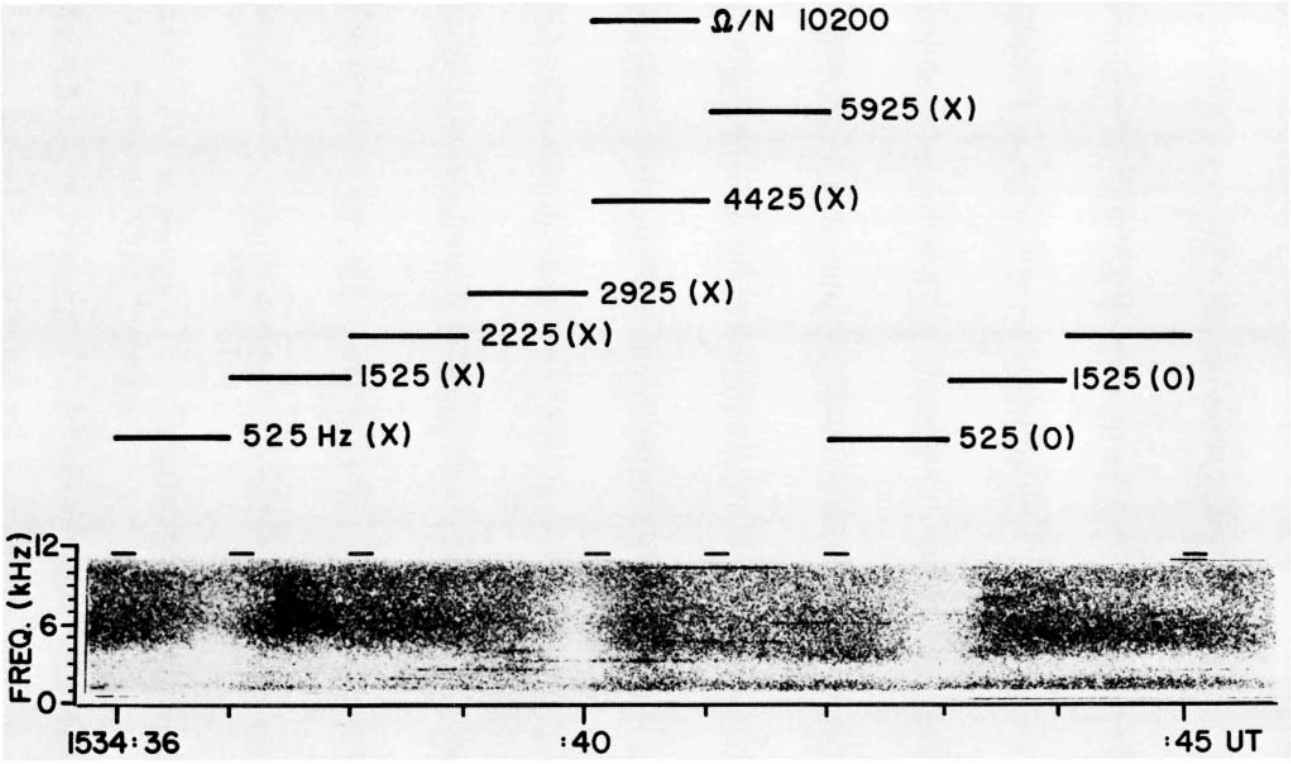

Fig. 2. Spectral film of 10-s segment of data record from DE 1 wideband receiver.

X mode is consistent with previous satellite observations of MPAe Heating [*James et al.*, 1984]. The absence of the signal at 525 Hz is due to the fact that the lower cutoff frequency of the wideband receiver is 600 Hz.

The ELF/VLF lines rise clearly above the broadband natural noise at many points across the 2-min observation period. This typically happens in the first half of the 12-s duty cycle of MPAe Heating when the HF polarization is X. At other times, hisslike noise masks the transmissions. The start and stop times of each pulse are not accurately measurable. The presence of rapid (250 μs) automatic gain control also contributed to the highly variable nature of the observed signal levels. Nevertheless, the delays of the beginning of each received pulse with respect to the known start of the corresponding transmitted pulse evidently amount to several hundred milliseconds. Also, it is clear that some pulses have greater lengths than the 1-s transmitted pulses. As will be discussed later, the bandwidth of the spectrum of each ELF line is broadened from less than 1 Hz at transmission to 10–20 Hz at reception.

The DE 1 wideband receiver also recorded transmissions from the Omega Norway VLF (Ω/N) navigational transmitter situated at Aldra, Norway (66°N, 13°E). The Ω/N transmission at 10.2 kHz, seen starting at about 40.3 s in Figure 2, exhibited pulse lengths of up to 1400 ms, compared with a transmitted length of 900 ms. Associated delays were a few to several hundred milliseconds. Hence it was confirmed that waves at slightly higher VLF frequencies from a nearby conventional transmitter exhibited pulse distortion similar to that seen in the MPAe transmissions.

The minimum delays of the Ω/N signals are smaller by 100–200 ms than those of the MPAe pulses. A ray-tracing evaluation of the delays associated with propagation in a smoothly varying medium, described below, showed that minimum delays of about 200 ms are expected. Because the Ω/N signals are stronger than the MPAe signals, it is reasonable to expect a weak, directly propagated component at DE 1 in addition to the stronger scattered components. Thus minimum delays on the relatively strong Ω/N pulses may be expected to be smaller than on the PEJ pulses, as observed.

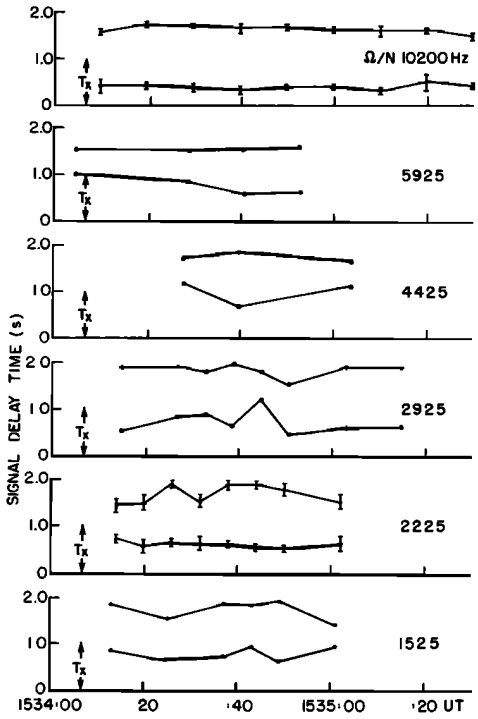

Fig. 3. History of the beginning and end of received pulses across the observation period for six observed lines. The start and end times of each identifiable pulse are each plotted as dots. The straight segments joining the dots show the general variation of the received pulse width. The arrows around "T_x" show the transmission time of each pulse. Typical reading uncertainties are indicated using error flags in a few cases.

3. Ray-Tracing Results and Comparison With Data

3.1. *Observed Delays*

We first compare the observed pulse lengths and delays with the predictions of ray tracing. The times of the leading and trailing edges of the ELF pulses, scaled by visual inspection of the spectral film record, are plotted in Figure 3. The plotted signal duration is the interval during which the pulse was visible above the strong background noise. Delays of the order of 1 s were systematically observed. The uncertainty in the measurements is indicated by the error bars.

The delays shown in Figure 3 range between 300 ms and 900 ms. The average time from the midpoint of the transmitted pulse to the midpoint of the received pulse lies in the range 700–800 ms. Comparison of the five MPAe lines reveals no obvious dependence of signal delay on frequency.

Several of the plotted pulses clearly have lengths significantly longer than the 1-s or 0.9-s emitted pulse length. Several others probably are longer than 1 s, but pulse limits are obscured by competing noise.

A first investigation was carried out to decide whether pulse delays and stretching could have been caused by multiple paths between the transmitter and the DE 1 receiver. To establish the propagation paths needed to explain the observations, ray tracing was used to find the signal delays predicted for propagation in a smooth ionosphere. The high-frequency waves at 2.759 MHz from MPAe Heating are assumed to propagate rectilinearly up to, and beyond, the assumed *E* layer source region at 100 km altitude. There, the HF waves create the ELF source in the auroral electrojet. The 30-km horizontal extent of the source, determined by the MPAe Heating beam width, is so small that the source can be treated as a point for the present analysis of signal delay. Propagation between the source and the satellite is computed using the cold-plasma dispersion relations [*Stix*, 1962] and the ray theory [*Haselgrove*, 1954]. With the ionospheric model set, there is a unique starting wave normal that produces the desired ray path.

A model of the ionosphere and magnetosphere was employed with the plasma frequency $f_{pe}(h)$ distribution shown in Figure 4. At the altitude h of the spacecraft, 10,970 km, f_{pe} was made to agree with the value of 58 kHz observed on DE 1 at 1534:00 UT. The values $f_{pe}(h = 300) = 6.0$ MHz and $f_{pe}(h = 100) = 1.5$ MHz were assigned on the basis of measurements made at the Kiruna, Sweden, ground ionosonde. The $f_{pe}(h)$ profile was given a Chapman layer form with a varying scale height above $h = 300$ km, and a parabolic form below 300 km. The density was assumed to

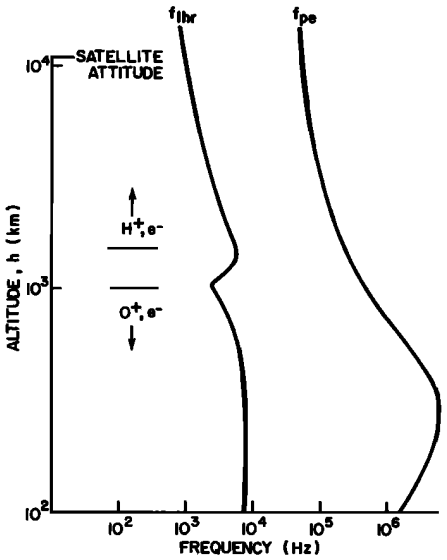

Fig. 4. (Right) The height profile $f_{pe}(h)$ of the electron plasma frequency. (Left) The resulting profile of the lower hybrid resonance frequency f_{lhr}.

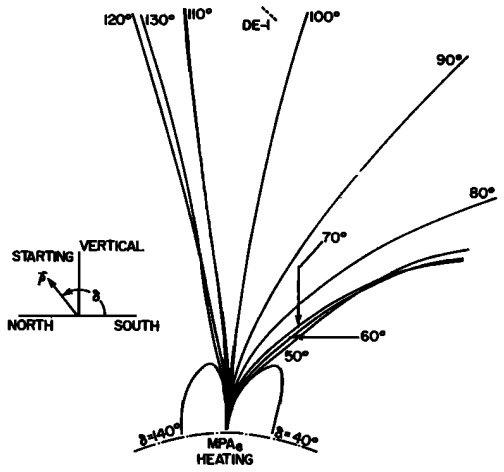

Fig. 5. Representative rays at 1525 Hz traced upward from the E region above MPAe Heating. The starting wave normals have elevations above the southward horizontal direction of δ and lie in the vertical north-south plane through MPAe Heating. The rays and the DE 1 orbit, shown as a dashed line, are projected onto the same plane.

be spherically stratified. The real terrestrial magnetic field $\mathbf{B}_0$ model was evaluated using the International Geomagnetic Reference Field (IGRF) 1980 coefficients [*Langel*, 1988]. The ion composition was assumed to change smoothly from pure O^+ at h = 1000 km to pure H^+ at h = 1500 km. The lower hybrid resonance frequency profile $f_{lhr}(h)$ consequently has extrema at 1000 km and 1400 km, as shown in Figure 4.

The above plasma model permitted an examination of the wave mode domains [*Stix*, 1962; *Gurnett et al.*, 1965; *Brice*, 1967] corresponding to the observed frequencies. For all frequencies 1525 $\leq f \leq$ 5925 Hz, waves would start propagating upward from 100 km in the right-hand-polarized mode above the local proton gyrofrequency and below the local f_{lhr}. At some point in the topside they would encounter the condition $f = f_{lhr}$. Above this height the propagation would remain in the right-hand-polarized mode, called the whistler mode. The six pulse frequencies shown in Figure 2 would all be received at DE 1 in the whistler mode.

3.2. *Ray-Tracing Predictions*

Rays traced upward from h = 100 km above MPAe Heating demonstrate the access of rays to the satellite locations. Figure 5 shows a selection of 1525-Hz rays traced upward in three dimensions projected onto the vertical geographic north-south plane including MPAe Heating. The starting wave normals $\boldsymbol{\rho}$ lie in the same plane and have varying elevations δ. The projection of the DE 1 path during 1534–1536 UT is shown as a dashed line.

Figure 6 is the similar result of three-dimensional ray tracing when the starting $\boldsymbol{\rho}$ vectors lie in the vertical east-west plane through MPAe Heating. The rays are projected onto this plane.

Figures 5 and 6 show that waves with low starting elevations reflect in the low topside ionosphere, in which case the $f = f_{lhr}$ condition is not encountered. At the higher starting elevations the propagation mode couples smoothly to the whistler mode, allowing access to DE 1.

Trial-and-error ray tracing between DE 1 and MPAe Heating was used to find the solution ray connecting them. For practical reasons it was more convenient to trace the rays downward from DE 1 toward the source target, a point 100 km above MPAe Heating. At the outset it was assumed that all starting three-dimensional wave normal directions allowed in the aforementioned cold-plasma mode at the satellite height were possible. A starting wave normal azimuth was chosen. A range of starting wave normal elevations were then used to start rays, and the starting wave normal elevation of the ray that passed closest to the target was noted. With the starting wave normal elevation held at this value, the starting azimuth was then swept to find the azimuth such that they ray made the closest approach to the target. This alternating procedure continued until a ray was

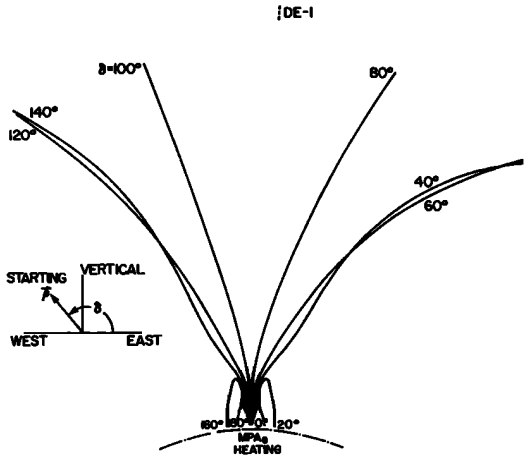

Fig. 6. Representative rays at 1525 Hz traced upward from the E region above MPAe Heating. The starting wave normals have elevations above the eastward horizontal direction of δ and lie in the vertical east-west plane through MPAe Heating. The rays and the DE 1 orbit, shown as a dashed line, are projected onto the same plane.

found that passed within 0.1° of the latitude and longitude of MPAe Heating at a height of 100 km. This was the required solution ray, with the understanding that the wave normal and group velocity directions had to be reversed to correspond to the actual direction of propagation from the source to the satellite.

The resulting group delays vary from 181 ms at 1525 Hz to 100 ms at 5925 Hz for the DE 1 position at 1534:30 UT. Over the same frequency range the values of the angle between the whistler mode wave normal and the magnetic field at the satellite location go from 16.4° to 17.3°, and the Doppler shift due to spacecraft motion varies from +0.09 to +0.20 Hz. The observed signal delays in Figure 3 significantly exceed the delays computed for direct propagation in a smooth ionosphere.

The importance to the calculated signal delay of the uncertainty in the ionospheric density distribution was estimated by tracing additional rays at 1525 Hz with the following changes: $f_{pe}(h = 300)$ was changed from 6 to 5 MHz in one case, and the O^+-H^+ transition range was changed from 1000–1500 km to 2000–2500 km in another case. The delays thus computed changed by 27 and 2 ms, respectively. Such changes are much less than the discrepancy between observed and theoretical signal delays.

The ELF modulation waveform on the HF carrier of Heating is expected to produce nonlinearly distorted ELF current waveforms during the *E* region heating process. The distortion leads to harmonics of the ELF modulating frequency [*James*, 1985]. However, the resulting radiated pulse at the ELF fundamental is expected to have a spectral width equal to the inverse pulse length, 1 Hz. Pulse dispersion of this 1-Hz spectrum during the smooth transionospheric propagation is negligible in comparison with the observed pulse stretching of hundreds of milliseconds.

3.3. *Upward Radiation From the Earth-Ionosphere Waveguide*

Measurements recorded on the ground near MPAe Heating indicated that the heater can strongly excite all the fundamental ELF/VLF frequencies and some of their harmonics. ELF/VLF energy can propagate from the PEJ through the Earth-ionosphere waveguide over distances of hundreds of kilometers [*Barr et al.*, 1986]. If this energy could cross the upper guide wall into the ionosphere, then a rather extensive area below an observing satellite could provide starting points for smooth upward propagation to the spacecraft.

During the observation period 1534–1536 UT the foot of the field lines through the spacecraft lay close to 77°N, 24°E, as can be seen in Figure 1. This appears to present an unfavorable geometry for the injection of waves from MPAe Heating lying 840 km southwest of the spacecraft field line foot. It appears unfavorable in the sense that even with waveguide propagation to the foot of the field line through the spacecraft, injected wave normals would not have the right elevation and azimuth for rays leading to the spacecraft. But because scattering at low altitudes could intervene to redirect waves toward the spacecraft, this possibility is evaluated below.

A study of the total *E* region that could irradiate the DE 1 satellite at a given time was determined by tracing rays from the spacecraft. Starting wave normals were allowed to vary through all elevations and azimuths. Rays with starting wave normals in or near the upper hemisphere propagated away from the Earth, some directly and others after reflection. The rays that were able to arrive at 100 km altitude defined the maximum extent of *E* region sources.

The *E* region zone thus determined is an almost circular zone of roughly 3000 km diameter, centered near the foot of the field line through the spacecraft. The signal delay for 1525 Hz lies between 180 ms and 200 ms for most of the connecting rays starting inside the zone. The delay rises to about 240 ms near the zone edges. Propagation inside the Earth-ionosphere waveguide adds up to about 10 ms delay. Thus injection into the ionosphere followed by smooth upward propagation to DE 1 accounts for no more than 250 ms delay, below the range of delays (300–900 ms) for the data shown in Figure 3. Pulse stretching in the case of the smooth magnetosphere cannot be greater than about 20 ms, as compared with the observed stretching of as much as 400 ms.

The main conclusion of the ray-tracing analysis is that propagation in a smooth magnetosphere does not account for the observed signal delays and pulse stretching.

4. PULSE SPECTRA

The spectra of the ELF/VLF lines provide further evidence in support of a scattering explanation of long signal delays and pulse stretching. We distinguish two limiting cases of propagation in the whistler mode: electromagnetic propagation entailing wave normal and group velocity directions within a few degrees of $\mathbf{B}_0$, and quasi-electrostatic propagation with wave normals separated from the resonance cone by a fraction of a degree. It seems unlikely that the observed long delays could be attributed to electromagnetic propagation because, with the group speeds near c, this would require propagation over total distances of the order of 100,000 km. It is difficult to conceive of a whistler mode ray path with this length constrained to start at MPAe Heating and end at the DE 1 location. We conclude that rising electromagnetic whistler mode waves are scattered into quasi-electrostatic waves with slow group speeds. This scattering would occur at heights where wave propagation is in the whistler mode, that is, between the $f = f_{lhr}$ altitude and the DE 1 altitude. The concept of scattering of electromagnetic whistler mode waves into quasi-electrostatic whistler mode waves has been discussed by *Bell and Ngo* [1988].

Figure 7 shows the ±10-dB shoulders of the ELF/VLF line spectra (solid lines) and the frequency of maximum signal strength (dashed line) in relation to the transmitted frequency (dotted line) of the ELF/VLF carrier. The points have been read from logarithmic amplitude spectra taken every 50 ms through the 1-s pulses. The data selected correspond to six of the strongest signals observed, including two cases of the Ω/N 10.2-kHz signal.

The line widths corresponding to the ±10-dB shoulders in Figure 7 range between 10 and 30 Hz, compared with the initial ELF/VLF line width of about 1 Hz. The peak frequency wanders between the spectral limits. On a few occasions the peak coincides with the transmitted carrier frequency, but in most cases the peak is well separated from the carrier. There is no obvious bias in the sign of the difference between the peak and the carrier. The overall impression is of a scattering process that leads to the

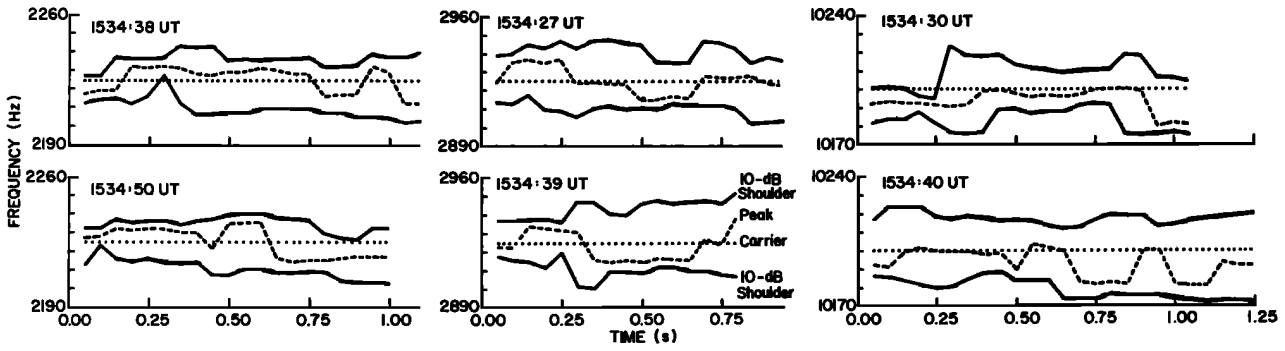

Fig. 7. Spectral shoulders at the points 10 dB below the maximum signal level (solid line), frequency of the maximum signal strength (dashed line), and transmitted carrier frequency (dotted line) for some observed lines. The labeled time is the UT of the start of the transmission. The abscissa scale is differential time.

observation of positive Doppler components one moment and negative components shortly after.

There is no evident difference between the MPAe and Ω/N line shapes. The Ω/N spectra are as asymmetric as the MPAe spectra. Similar Ω/N line shapes are maintained through the 2-min pass, suggesting that the scattering process occurs over a horizontal extent of at least a few hundred kilometers.

4.1. *Correspondence of Signal Delays and Line Widths*

The observed line widths can be shown to be consistent with the observed signal delays when interpreted as caused by Doppler broadening. Measurable Doppler shifts are detected by the satellite receiver due to the finite spacecraft speed and the finite wave numbers of the arriving ELF waves. As an example, consider the case of the 2925-Hz signals. These can propagate in the whistler mode from a height of 2700 km up to the spacecraft altitude, 10,973 km at 1534:40 UT. Suppose that at a point roughly halfway between these two heights ($h \simeq 7000$ km), fast electromagnetic whistler mode waves are scattered into relatively slow quasi-electrostatic waves. It is hypothesized that the scatterers produce quasi-electrostatic waves with a range of refractive index values. In the cold-plasma theory, a wide range of refractive index values can be obtained by exploring wave normal directions near the resonance cone.

Using the same cold-plasma ray-tracing procedure as described in section 2, rays at 2925 Hz were found which start at $h = 7000$ km and which terminate at the spacecraft location at 1534:40 UT such that their wave vectors $\mathbf{k}$ lie in the plane defined by $\mathbf{B}_0$ and the satellite velocity vector $\mathbf{v}_s$. This coplanarity guarantees that the resulting Doppler shift $f_D = -\mathbf{k}\cdot\mathbf{v}_s/2\pi$ is maximized. For rays that arrive at the satellite at 1533:40, the angle $(\mathbf{k}\cdot\mathbf{v}_s)$ is 27°.

A variety of rays was traced such that a range of f_D values at the spacecraft was obtained. When group delay d along the ray was plotted versus f_D, a relation was obtained which is very close to the linear relationship $d = 22.7/f_D$ for f_D values of the order of 10 Hz. According to this relationship, theoretical signal delays of hundreds of milliseconds correspond roughly to line widths of order of a few tens of hertz. This is what is observed and establishes a general consistency between the maximum group delays of several hundred milliseconds in Figure 3 and the maximum Doppler shifts in Figure 7 of a few tens of hertz.

The lower the frequency, the smaller the height range for whistler mode propagation. Figure 4 places the lower limit for 1525 Hz at $h = 6200$ km. Group and phase indices for 1525 Hz are similar to those found for 2925 Hz and allow the same conclusion about correspondence of observed delays and line widths.

The amplitude of quasi-electrostatic wave scattered by a density irregularity depends on the incident wave normal angle and the density enhancement of the irregularity [*Bell and Ngo*, 1988]. The fluctuations of the Doppler spectra in our Figure 7 imply that scattering geometries and irregularity densities varied randomly across the satellite pass. On this relatively short (2 min) pass, there was no obvious systematic change in the Doppler frequency spectrum with time implying a systematic change in the scattering geometry due to changing position of the spacecraft with respect to the source location. Also, we have no measurement of the irregularity density spectrum at the proposed height of scatter. So, although the present data are consistent with the linear scattering ideas of *Bell and Ngo* [1988], it is difficult to use the data to check the expected dependence of scattering on geometry.

4.2. *Harmonics*

The amplitude spectra upon which Figure 7 is based have a relative intensity calibration that permits intensity with respect to peak to be read to ±1 dB. Although not plotted, the 1525-Hz line also had peak values 10 dB above the background noise. The associated dynamic spectra gave no indication of a received line near 1575 Hz, the third harmonic of the 525-Hz modulation.

Theoretically, the radiating E region ELF currents are expected to have the spectrum of a 525-Hz rounded square wave. The harmonic ratio $I(525)/I(1575)$ could vary from 9.5 dB at relatively low D region altitudes to about 18 dB around 100 km [*James*, 1985].

Because the signal-to-noise ratios are about 15 dB, the absence of detectable 1575-Hz signals at DE 1 may be attributable to the competing ELF/VLF hiss in some of the observations. In the ISIS 1 satellite observations of *James et al.* [1984], the ratio $I(525)/I(1575)$ was of the order of 10 dB. Nevertheless, the complete absence of any trace of signal at 1575 Hz is surprising.

The intensity ratios measured on the ground are clearly different from both the theoretical predictions and the space observations. The measured ratio $I(1525)/I(1575)$ was found

to be 3–4.8 dB, where ground data closest in time (30 s) to the times plotted in Figure 7 were used. Also, the ratio $I(525)/I(1575)$ on the ground varied between 0.9 dB and 2.8 dB. During the ISIS satellite experiment this same ratio was observed to have an average value of 0.2 dB.

Thus in both the DE 1 and ISIS data the space and ground harmonic ratios are inconsistent, assuming a common source for both kinds of observed radiation. This inexplicable disparity points to a need for consideration of the excitation mechanism and of the role of the Earth-ionosphere waveguide.

4.3. *Signal Amplitudes*

It is instructive to compare the amplitudes of the MPAe PEJ and Ω/N pulses, considering that the latter comes from a "known" transmitter with which the "unknown" PEJ source efficiency can be calibrated. The logarithmic amplitude spectra from the wideband receiver show that the peaks of the most intense MPAe PEJ lines are about 10–15 dB above the surrounding broadband noise. Telemetered values of the automatic gain control were examined for the pulse periods in Figure 7; the input voltage corresponding to the frequency-integrated input power varied between 353 and 708 μV. Assuming that the 200-m dipole has an effective length of 100 m [cf. *Sonwalkar and Inan*, 1986], the total electric field E_t parallel to the dipole then lies between 3.5 and 7.0 μV/m. The effective noise field in the part of the total instrument bandwidth (10,000 Hz) occupied by the received line, of bandwidth $\Delta = 10$ Hz, is estimated to be $E_t(\Delta/10{,}000)^{1/2}$. If the line emission peak is 10 dB above this noise, then the peak field is $(10)^{1/2}E_t(10/10{,}000)^{1/2}$. This quantity lies between 0.36 and 0.70 μV/m for the four PEJ lines in Figure 7.

The Ω/N pulse intensity can be evaluated in a similar manner. During the period 1534:00–1535:00 the Ω/N level in the wideband receiver was 15–20 dB above the background when measured in a 100-Hz bandwidth. Assuming a constant, flat noise spectrum between the MPAe Heating frequency of 2925 Hz and the Ω/N frequency of 10,200 Hz, a signal/noise ratio of 15 dB then corresponds to a field of $(10^{1.5})^{1/2}E_t(100/10{,}000)^{1/2}$, lying between 2.0 and 4.0 μV/m.

The Ω/N field strengths at DE 1 are consistent with other satellite observations of ground VLF transmitters. FR 1 spacecraft overflights of a 20-kW transmitter operating at 16.8 kHz produced peak power recordings at $h = 750$ km of about 10^{-9} W/m^2 at night [*Aubry*, 1968]. The Kosmos 259 spacecraft also carried a VLF receiver which observed the spatial distribution of radiation from VLF transmitters at heights between 300 and 800 km [*Aksenov*, 1975]. At a height of about 4000 km above the Omega North Dakota 10-kW transmitter the DE 1 satellite recorded a peak power of 10^{-11} W/m^2 at dusk [*Inan et al.*, 1984]. In all of these observations the received power rolls off as a function of horizontal distance from the peak of its distribution. The rate lies in the range 1–4 dB per degree of latitude.

To a first approximation it is assumed that the two-dimensional distribution of whistler mode power flux injected into the ionosphere from a ground transmitter is mapped up along magnetic field lines, as the results of *Aubry* [1968] tend to show. The decrement of power flux at the DE 1 spacecraft from the peak power is determined by computing the great-circle geocentric angle subtended by Ω/N and the foot of the field line through DE 1, shown in Figure 1. At 1533:40 UT this angle is 14.8° and corresponds to a horizontal decrement of about 15 dB with respect to the peak power, using the values of *Inan et al.* [1984] as a lower limit. A power flux at DE 1 of $S_s = 10^{-12.5}$ W/m^2 results. Using the parallel-propagation assumption again, S_s is converted to wave electric field E_w with $S_s = \mu_p E_w^2/Z_0$, where Z_0 is the free-space impedance. Taking a value of 400 as a typical upper limit to the local phase refractive index μ_p required to produce the observed Doppler broadening at DE 1, $E_w = 0.6$ μV/m, which is similar to the Ω/N field strengths observed on DE 1. Hence, to the extent that agreement has been achieved between a simple model of the Ω/N radiation distribution in the ionosphere and the observations, this allows the Ω/N model to be used as a reference for estimating the PEJ source power.

The PEJ is equivalent to a radiator at *E* region heights having roughly 1/30 of the power of Ω/N referred to that point. The Ω/N transmitter radiates 10 kW isotropically [*CCIR*, 1986]. In the magnetically active auroral regions, as in the daytime conditions, the Ω/N waves suffer collisional absorption when crossing the ionospheric *D* region. Riometer measurements near Tromsø show a relatively modest absorption event at the time of the DE 1 pass. Assume 10 dB of auroral *D* region absorption [cf. *Inan et al.*, 1984]. Crudely, then, the PEJ equivalent isotropic radiator has a power of 10 dB below 10,000/30, or 30 W.

A smaller effective power would have resulted had we scaled the nighttime measurements of *Aubry* [1968] to the present circumstances. Given the local time and season of the present DE 1 pass, it seems best to apply the late afternoon peak value for S_s of *Inan et al.* [1984]. If this value of S_s is adjusted for the difference in transmitter powers, it does not differ much from *Aubry*'s [1968] daytime observations.

During the time of the MPAe observations, the linear wave receiver [*Shawhan et al.*, 1981] was operating in the 10 to 16-kHz mode and also detected the Ω/N transmissions. The linear wave receiver data were used to provide an independent check on received signal level. During the pass, the linear wave receiver was connected to a magnetic antenna, and its passband was 10–16 kHz, thus excluding the MPAe transmissions. Values of the wave magnetic field B_w between 4.7 and 15. × 10^{-3} pT were observed. Taking the geometric mean value of 8.4 × 10^{-3} pT and assuming parallel propagation with $\mu_p = 4$, we obtain $E_w \simeq cB_w/\mu_p = 0.6$ μV/m. The electromagnetic component of the Ω/N spectrum at DE 1 is thus seen to be somewhat weaker than the scattered quasi-electrostatic component.

On the other hand, if we choose a propagation direction close to the resonance cone with $\mu_p = 400$, say, then the elliptically polarized electric field of the wave has a semimajor axis of about 1/100 of the above E_w [*Bell et al.*, 1983]. Since the observed E_w strengths are much stronger, this supports the interpretation that the linear wave receiver detected only the electromagnetic component of the spectrum. We also note that the loop antenna connected to the linear wave receiver in this case is less sensitive (~14 dB for electromagnetic waves) than the long electric dipole used for the wideband receiver observations.

The PEJ line strengths observed in space can be compared with estimates of PEJ radiated levels detected on the ground. *Barr and Stubbe* [1984] calculated effective dipole moments

of 10–30 A km for the induced Hall currents around 1–3 kHz, using a theoretical model of the *E* region. *Barr et al.* [1986] reported that a point dipole with a moment of 30 A km is a good approximation to the ELF Hall current PEJ. This value is based on measurements made at a point 554 km from MPAe Heating but is consistent with typical magnetic field strengths of 1 pT measured on the ground 17 km away from the MPAe Heating.

Magnetic fields *B* measured on the ground near MPAe Heating during the present DE 1 pass varied between 2 and 6 pT in the range 1525–2925 Hz. Simply estimating the current *I* flowing in a straight conductor with $I = 2\pi rB/\mu_0$, we find that the *B* range corresponds to an *I* range of 1.0–2.5 A. If such currents are thought to flow across the heated region whose horizontal dimension is 30 km, the dipole moments then lie between 30 and 75 A km. These values are similar to previously reported values, and a representative value of 30 A km can be assumed.

Roughly speaking, the PEJ antenna carries currents of the order of 1 A and radiates a few tens of watts into the ionosphere. This analysis assumes that if free-energy sources intervened in the topside ionosphere to amplify the observed waves, the amount of amplification in the waves from the "known" source, Ω/N, was the same as in the waves from the "unknown" PEJ.

During the development of the auroral electrojet modulation technique an objective has been to evaluate the PEJ as an injector of ELF/VLF waves into the magnetosphere, for comparison with levels available from conventional ground transmitters with the same input power. The present work indicates that the PEJ as presently excited by MPAe Heating is not an efficient injector. The 1.5-MW HF transmitter has been shown to create a 30-W effective source and hence produce radiated levels inside the ionosphere/magnetosphere that are lower than those produced by a 10-kW conventional transmitter.

5. CONCLUSIONS

The signal delays and spectral widths of ELF and VLF waves radiated by the polar electrojet antenna (PEJ) and observed at a height of 11,000 km on the DE 1 satellite are consistent with a scattering process similar to that reported by *Bell and Ngo* [1988]. Ray tracing has been used to demonstrate that direct propagation from the *E* region PEJ results in signal delays significantly smaller than observed. Observed signal levels were around 0.4–0.7 μV/m.

These signal level results are quite different from those reported by *James et al.* [1984]. There, the spacecraft-observed ELF signal levels were high in comparison with what was expected with reference to ground-based observations. As distinct from ISIS, the DE 1 observations have no trace of radiation at harmonics of the fundamental ELF frequencies, even though MPAe Heating used a square-wave amplitude modulation, as in the ISIS experiment. In some of the present cases the wanted harmonics would be masked by the strong natural whistler mode hiss that filled much of the receiver bandwidth. However, analysis indicates that harmonics would have been detectable for a number of 525-Hz pulses if their intensities were higher than 15 dB below the fundamental.

Acknowledgments. We are grateful to D. A. Gurnett for the use of the wideband receiver data. The MPAe Heating project was supported by the Deutsche Forschungsgemeinschaft. The Dynamics Explorer research work at Stanford is supported by the National Aeronautics and Space Administration grant NAG5-476.

The Editor thanks J. L. Green and J. D. Menietti for their assistance in evaluating this paper.

REFERENCES

Aksenov, V. I., Investigation of the propagation of very long radio waves in the earth's ionosphere, II, Results of experiments with the Kosmos-142 and Kosmos-259 artificial satellites, *Radiophys. Quantum Electron.*, Engl, Transl., *18*, 996–1001, 1975.

Aubry, M. P., Some results of the FR-1 satellite experiment on the VLF wave field in the zone close to the transmitter, *J. Atmos. Terr. Phys.*, *30*, 1161–1182, 1968.

Barr, R., and P. Stubbe, ELF and VLF radiation from the "polar electrojet antenna," *Radio Sci.*, *19*, 1111–1122, 1984.

Barr, R., P. Stubbe, M. T. Rietveld, and H. Kopka, ELF and VLF signals radiated by the "Polar Electrojet Antenna": Experimental results, *J. Geophys. Res.*, *91*, 4451–4459, 1986.

Bell, T. F., and H. D. Ngo, Electrostatic waves stimulated by coherent VLF signals propagating in and near the inner radiation belt, *J. Geophys. Res.*, *93*, 2599–2618, 1988.

Bell, T. F., H. G. James, U. S. Inan, and J. P. Katsufrakis, The apparent spectral broadening of VLF transmitter signals during transionospheric propagation, *J. Geophys. Res.*, *88*, 4813–4840, 1983.

Brice, N. M., Ion effects observed in radio wave propagation in the ionosphere, in *Electromagnetic Wave Theory*, part 1, edited by J. Brown, pp. 197–209, Pergamon, New York, 1967.

CCIR, International Radio Consultative Committee, *Recommendations and Reports of the CCIR*, vol. 7, *Standard Frequencies and Time Signals*, *16th Plenary Assembly*, *Dubrovnik*, International Telecommunication Union, Geneva, 1986.

Gurnett, D. A., and U. S. Inan, Plasma wave observations with the Dynamics Explorer 1 spacecraft, *Rev. Geophys.*, *26*, 285–316, 1988.

Gurnett, D. A., S. D. Shawhan, N. M. Brice, and R. L. Smith, Ion cyclotron whistlers, *J. Geophys. Res.*, *70*, 1665–1688, 1965.

Haselgrove, J., Ray theory and a new method for ray tracing, in *The Physics of the Ionosphere*, pp. 355–364, Physical Society, London, 1954.

Inan, U. S. and R. A. Helliwell, Active experiments from ground, in *Results of the Arcad 3 Project and of Recent Programmes in Magnetospheric and Ionospheric Physics Toulouse 84*, pp. 599–607, Cepadues-Editions, Toulouse, France, 1985.

Inan, U. S., H. C. Chang, and R. A. Helliwell, Electron precipitation zones around major ground-based signal sources, *J. Geophys. Res.*, *89*, 2891–2906, 1984.

James, H. G., The ELF spectrum of artificially modulated *D/E*-region conductivity, *J. Atmos. Terr. Phys.*, *47*, 1129–1142, 1985.

James, H. G., R. L. Dowden, M. T. Rietveld, P. Stubbe, and H. Kopka, Simultaneous observations of ELF waves from an artificially modulated auroral electrojet in space and on the ground, *J. Geophys. Res.*, *89*, 1655–1666, 1984.

Langel, R. A., International Geomagnetic Reference Field revision 1987, *Eos Trans. AGU*, *69*, 557–558, 1988.

Lefeuvre, F., et al., Detection from Aureol-3 of the modulation of auroral electrojet by HF-heating from ELF signals in the upper atmosphere above Tromsoe, in *Results of the Arcad 3 Project and of Recent Programmes in Magnetospheric and Ionospheric Physics Toulouse 84*, pp. 609–619, Cepadues-Editions, Toulouse, France, 1985.

Rietveld, M. T., P. Stubbe, and H. Kopka, On the frequency dependence of ELF/VLF waves produced by modulated ionospheric heating, *Radio Sci.*, *24*, 270–278, 1989.

Shawhan, S. D., D. A. Gurnett, D. L. Odem, R. A. Helliwell, and C. G. Park, The plasma wave and quasi-static electric field instrument (PWI) for Dynamics Explorer-A, *Space Sci. Instrum.*, *5*, 535–550, 1981.

Sonwalkar, V. S., and U. S. Inan, Measurements of Siple transmitter signals on the DE 1 satellite: Wave normal direction and effective antenna length, *J. Geophys. Res.*, *91*, 154–164, 1986.

Stix, T. H., *The Theory of Plasma Waves*, 283 pp., McGraw-Hill, New York, 1962.

Stubbe, P., et al., Ionospheric modification experiments with the Tromsø MPAe Heating facility, *J. Atmos. Terr. Phys.*, *47*, 1151–1163, 1985.

Titova, E. E., V. I. Di, V. E. Yurov, O. M. Raspopov, V. Yu. Traktengerts, F. Jiricek, and P. Triska, Interaction between VLF waves and turbulent ionosphere, *Geophys. Res. Lett.*, *11*, 323–326, 1984.

U. S. Inan, Space, Telecommunications and Radioscience Laboratory, Department of Electrical Engineering/SEL, Stanford University, Stanford, CA 94305.

H. G. James, Communications Research Centre, 3701 Carling Avenue, P. O. Box 11490, Station "H," Ottawa, Ontario, Canada K2H 8S2.

M. T. Rietveld, EISCAT, N9027 Ramfjordbotn, Norway.

(Received December 29, 1989;
revised April 16, 1990;
accepted April 16, 1990.)